GEOLOGY | THE GEOLOGICAL SOCIETY OF AMERICA®

https://doi.org/10.1130/G47451.1

Manuscript received 27 November 2019
Revised manuscript received 28 February 2020
Manuscript accepted 28 February 2020

Tidal modulation of river-flood deposits: How low can you go?

Vittorio Maselli[1], Alexandre Normandeau[2], Michael Nones[3], Tommaso Tesi[4], Leonardo Langone[4], Fabio Trincardi[5] and Kevin M. Bohacs[6]

[1]Department of Earth and Environmental Sciences, Dalhousie University, Halifax, Nova Scotia B3H 4R2, Canada
[2]Geological Survey of Canada (Atlantic), Bedford Institute of Oceanography, Dartmouth, Nova Scotia B2Y 4A2, Canada
[3]Department of Hydrology and Hydrodynamics, Institute of Geophysics, Polish Academy of Sciences, 01-452 Warsaw, Poland
[4]Institute of Polar Sciences, Consiglio Nazionale delle Ricerche (CNR), Bologna, 40129, Italy
[5]Institute of Marine Sciences, Consiglio Nazionale delle Ricerche (CNR), Bologna, 40129, Italy
[6]KMBohacs GEOconsulting LLC, Houston, Texas 77042, USA

ABSTRACT

Quantification of the interaction between river discharge and tides is vital to characterize fluvio-deltaic systems, to identify diagnostic elements of tidal signatures in the rock record, and to reconstruct paleogeographies. In modern systems, even microtides can significantly influence delta morphodynamics; yet, many fundamental processes, particularly in prodeltaic settings, remain elusive. Here, by combining a unique process-product data set acquired during a flood event of the Po River (Italy) with numerical modeling, we show that tidal signatures are recorded in the open-water prodelta zone of a microtidal system. Based on the analyses of box-cores collected before and after a flood off the main distributary channel, we interpreted storm beds, tide-modulated flood strata of alternating normal and inverse graded beds, and rapid bioturbation. Modeling of the river discharge indicates that, at the peak of the flood, the steepening of the water-surface profile forced by 0.15 m lowering of sea level during low tides generated an 8% increase in river flow velocity. The alternation of profile steepness and associated cyclicity in flow strength during consecutive tidal cycles controlled the sediment load of the plume and, consequently, led to the deposition of tidal-modulated strata. Formation of microtidal signals appears to be enhanced in fluvio-deltaic successions characterized by multiple distributaries and in basins where river floods are out of phase with storm-wave activity. Bioturbation of sediment, which can start during the waning stage of the flow, and erosion by storm waves hamper the preservation of tidal signals, unless rapid burial occurs. The recognition of tidal-modulated strata in river-dominated settings may facilitate the characterization of mudstone reservoirs and reconstruction of paleogeographic conditions during deposition.

INTRODUCTION

Tide-influenced or tide-dominated fluvio-deltaic systems normally develop in the presence of macro- and mesotidal regimes, or where the tidal prism is large enough with respect to the cross-sectional area through which the water flows to generate fast tidal currents (chapter 9 *in* James and Dalrymple, 2010). Modern systems such as the Fly River Delta (Papua New Guinea), Schelde Delta (Netherlands), and Cobequid Bay–Salmon River (Canada) have been investigated to describe tidal sedimentary facies and subenvironments (Dalrymple et al., 2003; Dalrymple and Choi, 2007), and to develop interpretive models for the rock record (Longhitano et al., 2012). Geological evidence of the interaction between river discharge and tidal dynamics can be recorded by both large- and small-scale features across the fluvial-to-marine transition zone (FMTZ) to the prodelta. Diagnostic elements span from variations in channel morphology (Gugliotta and Saito, 2019) to sedimentary structures (Jaeger and Nittrouer, 1995; Peng et al., 2018). At the seaward limit of the FMTZ, where tidal currents are stronger, increasing rates of river discharge progressively reduce tidal current speed (Dalrymple and Choi, 2007). Consequently, tidal signals in river flood deposits are best preserved during the waning stage of floods or in the presence of large tidal prisms compared to river discharge (Dalrymple et al., 2015; Olariu et al., 2015). Examples of both conditions have been interpreted in the Campanian Neslen Formation, Utah, USA (Dalrymple et al., 2015; Olariu et al., 2015). Microtidal oscillations, however, may largely affect current velocity and consequently the morphodynamics of deltas (Shaw and Mohrig, 2014; Hanegan and Georgiou, 2015; Rossi et al., 2016). Prodeltaic settings have low to negligible river currents and should be well suited to record tidal signals, even in river flood strata. Despite tidal rhythmites inferred in ancient prodeltaic strata (Williams, 1991), these tidally "modulated" facies have not been confirmed in modern settings.

By integrating a unique process-product data set with numerical modeling, we demonstrate with unprecedented detail that extremely small tidal ranges (i.e., <1 m) can modulate river discharge sufficiently to control flood deposition in prodeltaic settings.

REGIONAL SETTING

The mean annual discharge of the Po River at Pontelagoscuro, Italy (Fig. 1A), is ~1500 m^3/s, with peak discharges >12,000 m^3/s. The Pila and Tolle distributary channels supply 60% and 12%, respectively, of the total water and sediment discharge of the Po River (Fig. 1A; Syvitski et al., 2005). Spring and neap tides in the northern Adriatic Sea have amplitudes of ~86 cm and 20 cm, respectively. At the Pila channel, the flux is reversed during flood tide, when river discharge is <1000 m^3/s (Maicu et al., 2018). Seasonal Po River floods typically reach the sea during fair-weather conditions (Wheatcroft et al., 2006).

METHODS

Field data were collected in April–May 2009 during a rapid-response cruise (Tesi et al., 2011) that investigated a flood event (peak of ~8000 m^3/s at Cavanella, recurrence time of

CITATION: Maselli, V., et al., 2020, Tidal modulation of river-flood deposits: How low can you go?: Geology, v. 48, p. , https://doi.org/10.1130/G47451.1

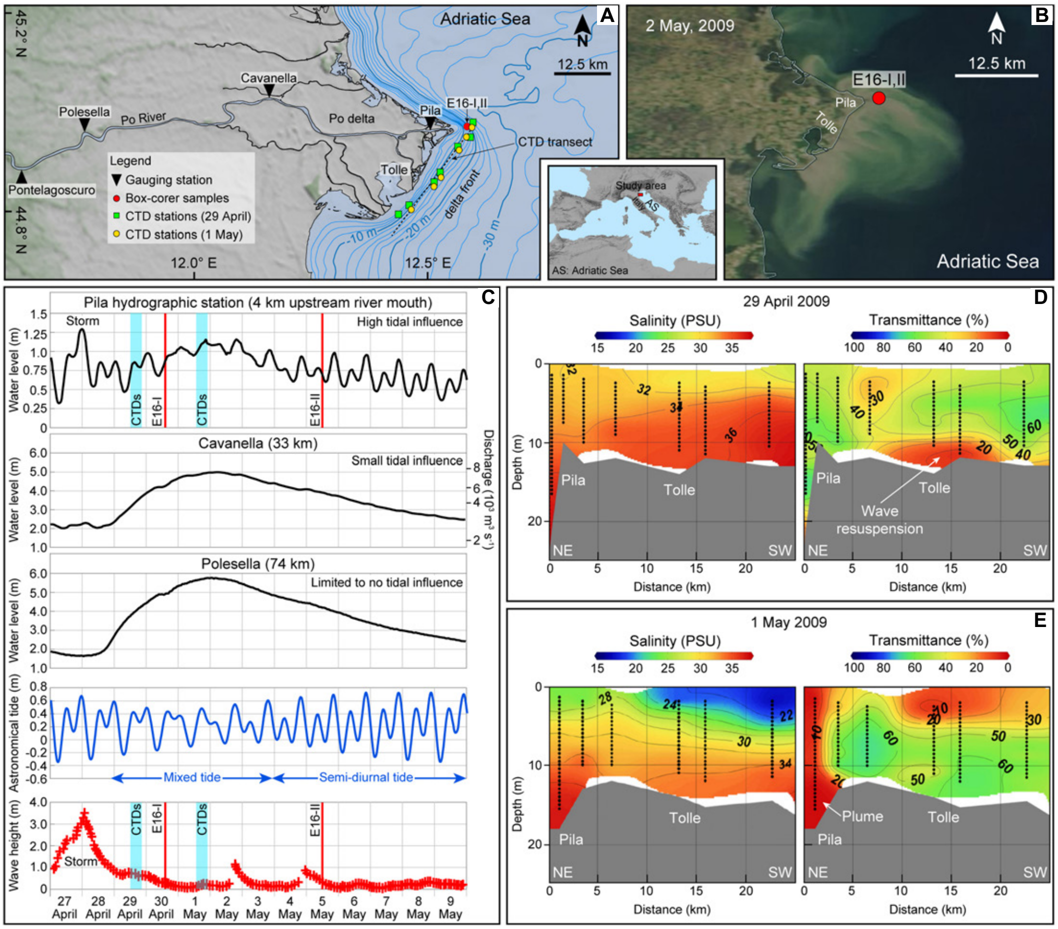

Figure 1. (A) Study area (Po River, Italy) with locations of hydrographic stations, conductivity-temperature-depth (CTD) profiles, and E16 coring site. (B) Satellite image of the Po River flood on 2 May 2009. (C) Measured Po River surface-water elevations (black lines), with timing of CTD and box-corer sampling, and predicted astronomical tidal amplitude (blue) and wave heights (red) off the Pila distributary mouth. (D, E) Salinity and transmittance profiles (modified from Tesi et al., 2011).

50–70 yr) of the Po River, Italy (Fig. 1). See the GSA Data Repository[1] for details on data acquisition, processing, and modeling. Conductivity-temperature-depth (CTD) profiles along with light transmittance data and suspended sediment concentrations (SSCs) were acquired on 29 April and on 1 May (flood peak) on transects parallel to the coastline (Fig. 1A). Box-cores E16-I and E16-II were collected at ~16 m water depth from the same location offshore the mouth of the Pila distributary channel on 30 April and on 5 May, respectively (Figs. 1 and 2). A slab of sediment orthogonal to the layering was extracted on deck from each box-core, kept in a cold room (4 °C), and X-rayed in laboratory after 10 d. The evolution of the water profile and bed shear stress was numerically simulated using the one-dimensional model Hec-Ras 5.0.7 (https://www.hec.usace.army.mil/software/hec-ras/; Brunner, 2016).

[1]Supplemental Material. Data acquisition and processing, numerical modelling set-up, calibration, and results. Please visit https://doi.org/10.1130/GEOL.26213S.12091686 to access the supplemental material, and contact editing@geosociety.org with any questions.

RESULTS

The water level at Cavanella began to rise the night of 28 April, peaked on 1 May, and waned for 10 d (Figs. 1A and 1C). A storm preceded the flood on 27–28 April and generated >3-m-high waves (Fig. 1C), with modeled bottom orbital velocities up to 140 cm/s at 20 m water depth (Bertotti and Cavaleri, 2009).

On 29 April, salinity profiles showed no freshwater plume in the prodelta region offshore the Pila and Tolle distributary mouths (Fig. 1D). Transmittance was high offshore the Pila channel (Fig. 1D), and low SSCs characterized both surface (5.68 ± 0.3 mg/L) and bottom (2.72 ± 0.72 mg/L) waters. Offshore the mouth of the Tolle channel, surface waters had high measured light transmittance and low SSC (3.04 ± 0.54 mg/L), while bottom waters had much lower transmittance and higher SSC (13.21 ± 2.1 mg/L).

The X-radiograph of box-core E16-I, collected before peak flooding, showed a 2-cm-thick layer at the top, with internal cross-laminae that unconformably overlay older bioturbated sediments (Fig. 2). This upper layer was characterized by high X-ray attenuation (denser sediment) compared to the underlying strata, which showed a diverse suite of physical (e.g., laminae, lenticular bedding, soft-sediment deformation) and biogenic sedimentary structures. Two other layers with high X-ray attenuation occurred at depths of 11 and 19 cm (Fig. 2).

On 1 May, surface waters had overall lower salinities, particularly offshore the Tolle distributary (Fig. 1D), and a plume of river-derived sediments flowed across the prodelta region. At station E16, the transmissometer recorded 0% light transmission, and both surface and bottom waters showed their highest SSCs, with values of 53.41 ± 4.77 mg/L and 24.35 ± 0.21 mg/L, respectively. A second plume of sediment flowed from the mouth of the Tolle channel, remaining confined to surface waters (Fig. 1D). Off Tolle, SSCs were 26.51 ± 1.05 mg/L and 10.01 ± 0.74 mg/L in surface and bottom waters, respectively.

The X-radiograph of box-core E16-II shows (1) a 5-cm-thick basal layer (22–17 cm) characterized by an upward decrease in X-ray attenuation, moderate bioturbation, and a D_{50} (average grain size) of ~6 µm (Fig. 2); a 3-cm-thick and high-attenuation layer (17–14 cm) with cross-laminae, sparse bioturbation, unimodal grains with D_{50} up to 36 µm, and sharp upper and lower contacts; a 14-cm-thick upper interval (14–0 cm) characterized by cyclic changes in X-ray attenuation, with 5 dark (K) layers alternating with 5 light (L) ones (Fig. 2). Each

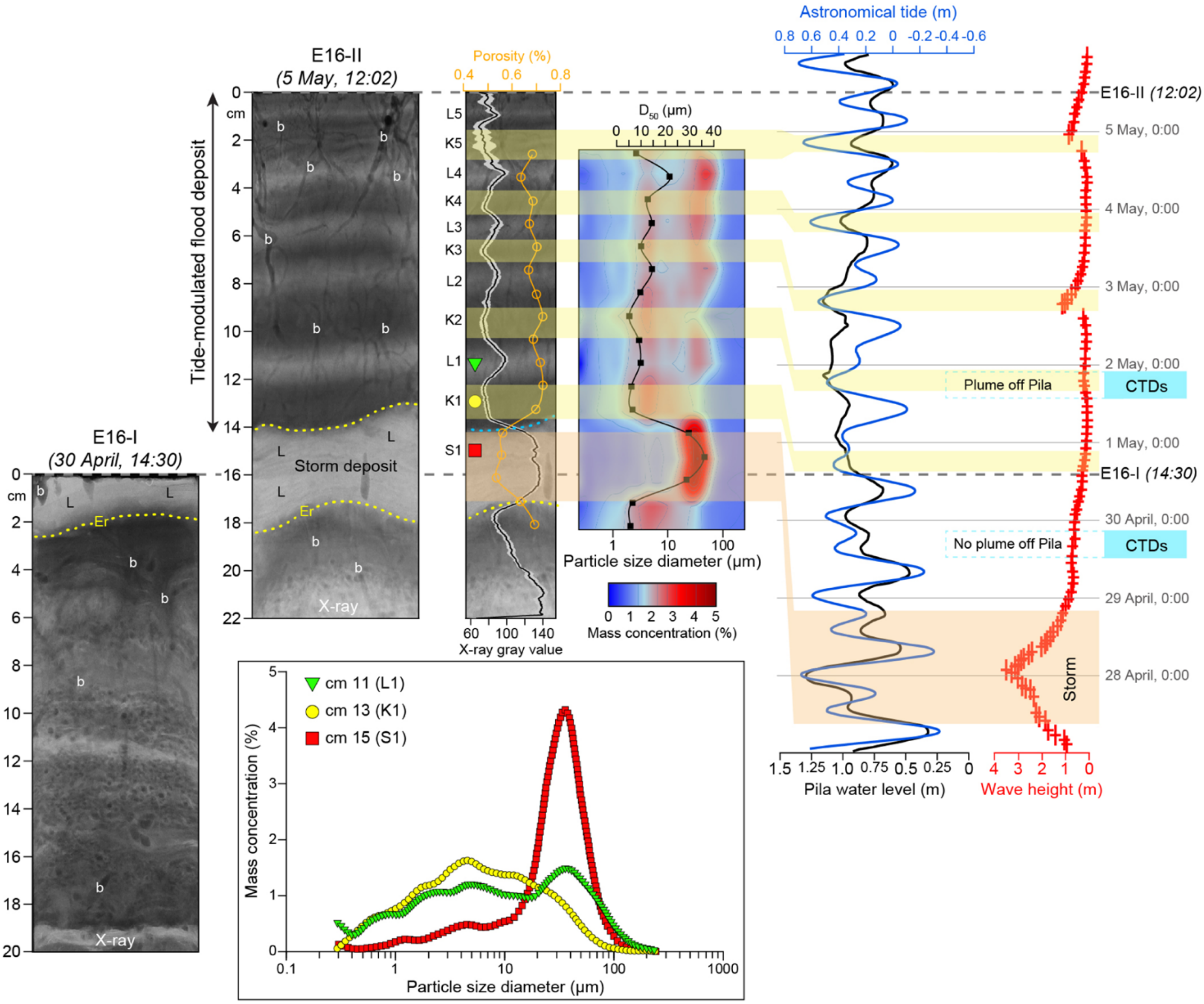

Figure 2. Core description related to coeval river, tide, and wave conditions on the Po River, Italy. X-radiographs of box-corer samples E16-I and E16-II (b—bioturbation, L—cross-laminae), porosity, grain-size analyses of E16-II. Dark and finer-grained intervals (K1 to K5) formed during high tides are highlighted by yellow bars. Predicted astronomical tidal amplitudes (blue) and wave heights (red) off the Pila distributary mouth, with the timing of sampling for conductivity-temperature-depth (CTD) profiles and box-cores. Particle size distributions of intervals S1, K1, and L1.

layer showed gradational changes in attenuation at both the lower and upper contacts; no clear erosional surfaces or sedimentary structures due to traction were visible at the core scale. Ongoing bioturbation was visible soon after the subsampling through the slab. The grain-size analyses showed poorly sorted, multimodal sediment distributions with D_{50} of 5 μm (D_{90} = 32 μm) for K layers and D_{50} of 12 μm (D_{90} = 75 μm) for L layers. An overall coarsening-upward trend was visible in the 14 cm interval (Fig. 2). The grain size from the 3-cm-thick S1 layer showed, conversely, a well-sorted deposit, lacking fine-grained sediments but enriched in coarser sizes, with a peak frequency distribution at 40 μm (Fig. 2).

DISCUSSION

Event Stratigraphy: Storm and Flood Deposits

When E16-I was recovered, the peak of the flood had not occurred, and CTD data do not show a sediment plume flowing across the prodelta (Figs. 1C and 2). Yet, the X-radiograph of E16-I contains a 2-cm-thick coarse deposit at the top (Fig. 2). In E16-II, a 3-cm-thick deposit with the same character (basal erosional contact and cross-laminae) is visible above a depth of 17 cm, suggesting that the layer may represent the same event at the top of E16-I. Because a river-derived plume was not present in surficial or bottom waters at the time this layer was deposited (Fig. 1D), it is unlikely to have resulted from river discharge. E16-I was, however, collected 2 d after the 27–28 April storm that generated >3-m-high waves (Fig. 1C). High SSC and low transmittance in bottom waters off the mouth of the Tolle channel on 29 April are, consequently, interpreted as having been generated by sediment resuspension due to the storm waves (Fig. 1D), and the coarse layer observed in E16-I is interpreted as the result of in situ reworking by direct wave stress or of a wave-enhanced sediment-gravity flow (WESGF; Macquaker et al., 2010). A WESGF with near-bed concentrations of 10–50 g/L decreasing to 0.2–3 g/L at 10 cm above seabed was observed offshore the Tolle channel in a water depth of 13 m during a previous storm with 3.8 m significant wave

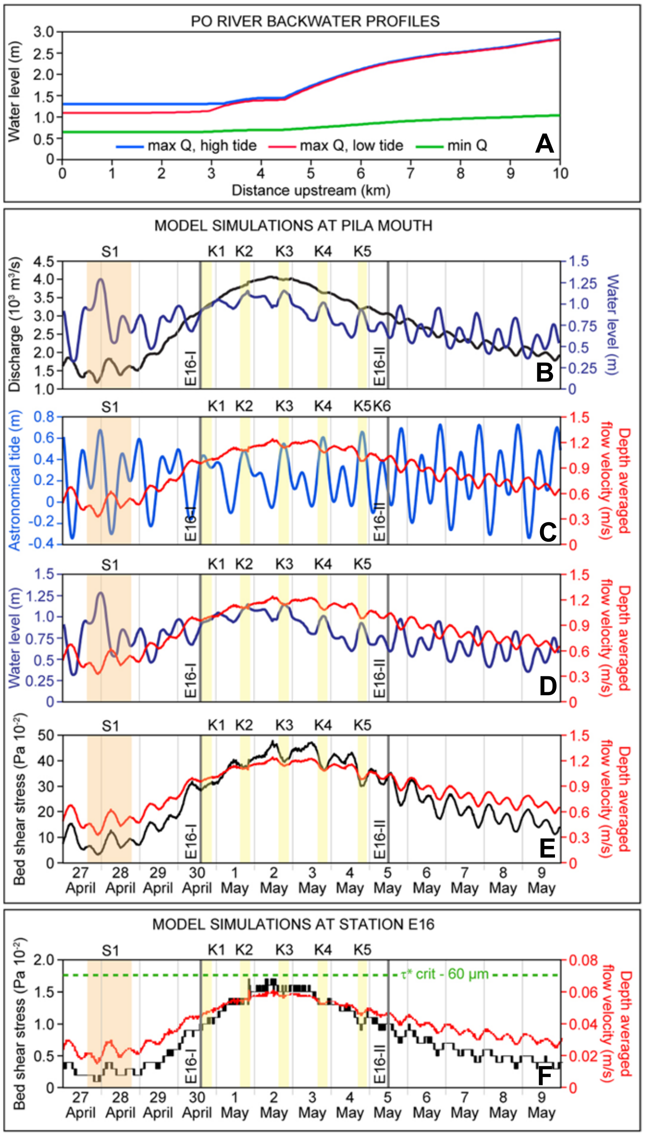

Figure 3. (A) Simulated surface-water elevations show M2 drawdown profiles for peak discharge at high (blue line) and low (red line) tide, and low-flow conditions (Q = 1000 m³/s; green line). (B–E) Model simulations of discharge, tidal amplitude, water level, bed shear stress, and flow velocity at the mouth of the Pila distributary channel. (F) Model simulation of bed shear stress and flow velocity at station E16, with critical shear stress (τ* crit) for 60 µm. Storm layer S1 is in orange, and finer-grained intervals (K1–K5) of the flood deposit are in yellow.

height (Traykovski et al., 2007). Since the 27–28 April storm had similar wave heights, and the seafloor offshore the Pila channel is steeper than that offshore the Tolle channel, a WESGF likely occurred. The lack of continuous in situ observations during this study, however, prevents further discussion. The 14-cm-thick bed above S1 in E16-II is interpreted as representing a different event: a flood deposit accumulated between 30 April and 5 May, during peak flooding and early waning stages (Figs. 1D and 2). The ^{7}Be profiles (see supplementary material) indicate the recent deposition of both event layers, but they do not differentiate their timing.

The flood deposit has alternating coarser (L1–L5) and finer (K1–K5) layers (Fig. 2). The gradational contacts between layers, the lack of sedimentary structures, and the poorly sorted nature of the sediments suggest that deposition was driven by settling of particles in suspension promoted by salt-driven flocculation, a dominant sedimentation mechanism in the Po River Delta (Fox et al., 2004; Milligan et al., 2007). This interpretation agrees with CTD data collected on 1 May that showed a freshwater plume mixing with the seawater and resulting in a turbid plume extending down to the seabed (Fig. 1E). On top, cyclic variations in sediment grain size imply that other mechanisms controlled turbid plume dynamics, sediment content, and settling, such as tides.

Tidal Modulation of a Flood Deposit

Because no storms occurred during the accumulation of the flood deposit and no oscillations in the river discharge were detected at stations located upstream of the backwater influence, tides are the most likely mechanism to explain the cyclic variation in silt content. This hypothesis is corroborated by the correspondence between the number of fine-grained layers and number of high tides that occurred between the collection of the two cores (Fig. 2).

To test whether tides were indeed responsible for cyclic deposition during the flood, we ran a simple one-dimensional numerical model of the Po River discharge (Fig. 3). The flow simulated at the Pila mouth is always unidirectionally seaward during the river flood, in agreement with Maicu et al. (2018). Because the steepness of the water profile is directly proportional to the flow velocity (Lamb et al., 2012), low tides force higher flow velocity. This is confirmed by comparing depth-averaged flow velocities at the river mouth with astronomical tides and water levels (Fig. 3). At the Pila distributary mouth during the peak of the flood (Fig. 3B), the simulated river flow velocity was 1.2 m/s, and tidal water-level oscillations of ~0.15 m generated a change of ~0.1 m/s (Figs. 3C–3E). Although such velocity variations are small (~8% of river flow velocity), microtides influenced river hydraulics and the sediment load of the plume. Model results also indicate that the critical bed shear stress for a grain size of 60 µm, the lowest value in the model, is never reached at the location of the core on the prodelta (Fig. 3F), in agreement with the lack of traction structures in core E16-II. The small coarsening-up trend visible in the flood deposit (Fig. 2) may reflect increasing availability of coarser sediments produced by erosion of the riverbed, or bioturbation.

Formation, Preservation Potential, and Implications of Tide-Modulated Flood Deposits

River floods that last for several days and supply abundant sediment are prerequisite features for recording tidal signals in prodeltaic deposits. Tidally modulated flood strata are more likely to occur in fluvio-deltaic systems with distributary channels, as the peak discharge is divided among distributary mouths, thus increasing the relative influence of tidal flow (Dalrymple et al., 2015). The rapid burial associated with the deposition during the waning stage of the flow, when sediment is still being supplied quickly, enhances signal preservation by reducing the transit time through the mixing zone (Bentley et al., 2006). Conversely, microtidal signals in prodeltaic successions can be obscured during deposition if the flood reaches the basin during a storm, or they can be disrupted by postdepositional processes like storm waves and bioturbation (Bentley and Nittrouer, 2003). In the study area, river floods and storms occur at different times, which favor tidal signal preservation (Wheatcroft et al., 2006). Bioturbation was visible in E16-II shortly after sampling, which indicates that it occurred exceptionally quickly, during the waning phase of the flood (Wheatcroft et al., 2006). The extensive bioturbation visible on the X-ray image, however, likely formed during the time elapsed between sampling and X-ray scanning.

Tide-modulated flows potentially transport coarser grains farther away from river mouths than do purely river-dominated flows (Bohacs et al., 2014), affecting the distribution of potential hydrocarbon carrier beds or leak pathways. Strata interpreted as formed by tide-modulated flows suggest different environmental and paleogeographic conditions than those for purely river-generated hyperpycnites. Recognition of subtle tidal influence will assist in the characterization of hydrocarbon sources, unconventional/mudstone reservoirs, and seal properties and can support the diagnosis of shelfal parasequence types (Bohacs, 1998; Passey et al., 2010; Bohacs et al., 2013, 2014).

CONCLUSIONS

Our study is the first to observationally and numerically link the microtidal modulation of river flood discharge to laminated flood strata in a modern prodeltaic setting. We show how microtides control river hydraulics and sediment transport in the prodelta, thus demonstrating that tidal signals are not only associated with macro- and mesotidal settings, but also with certain river-dominated ones, as suggested by Dalrymple and Choi (2007). Our results can help to interpret sedimentary signals preserved in ancient prodeltaic sequences and facilitate evaluation of the climatic regime of the basin and its bearing on the timing of river floods.

ACKNOWLEDGMENTS

This research was undertaken thanks in part to funding from the Canada First Research Excellence Fund, through the Ocean Frontier Institute. The work done by Michael Nones was supported within statutory activities no. 3841/E-41/S/2020, Ministry of Science and Higher Education of Poland, and by the Polish National Agency for Academic Exchange under Grant No. PPI/PZA/2019/1/00107/U/00001. We thank the editor, and reviewers Ron Steel, Robert Dalrymple, and Samuel Bentley for their positive and constructive comments.

REFERENCES CITED

Bentley, S.J., and Nittrouer, C.A., 2003, Emplacement, modification, and preservation of event strata on a flood-dominated continental shelf: Eel shelf, northern California: Continental Shelf Research, v. 23, p. 1465–1493, https://doi.org/10.1016/j.csr.2003.08.005.

Bentley, S.J., Sheremet, A., and Jaeger, J.M., 2006, Event sedimentation, bioturbation, and preserved sedimentary fabric: Field and model comparisons in three contrasting marine settings: Continental Shelf Research, v. 26, p. 2108–2124, https://doi.org/10.1016/j.csr.2006.07.003.

Bertotti, L., and Cavaleri, L., 2009, Wind and wave predictions in the Adriatic Sea: Journal of Marine Systems, v. 78, p. 227–234, https://doi.org/10.1016/j.jmarsys.2009.01.018.

Bohacs, K.M., 1998, Contrasting expressions of depositional sequences in mudrocks from marine to non marine environs, *in* Schieber, J., Zimmerle, W., and Sethi, P., eds., Mudstones and Shales; Characteristics at the Basin Scale: Stuttgart, Germany, Schweizerbart'sche Verlagsbuchhandlung, v. 1, p. 32–77.

Bohacs, K.M., Passey, Q.R., Rudnicki, M., Esch, W.L., and Lazar, O.R., 2013, The spectrum of fine-grained reservoirs from 'shale gas' to 'shale oil'/tight liquids: Essential attributes, key controls, practical characterization: Proceedings of the International Petroleum Technology Conference: Beijing, China, paper 16676.

Bohacs, K.M., Lazar, O.R., and Demko, T.M., 2014, Parasequence types in shelfal mudstone strata—Quantitative observations of lithofacies and stacking patterns, and conceptual link to modern depositional regimes: Geology, v. 42, p. 131–134, https://doi.org/10.1130/G35089.1.

Brunner, G.W., 2016, HEC-RAS, River Analysis System: Hydraulic Reference Manual, Version 5.0: Davis, California, U.S. Army Corps of Engineers Hydrologic Engineering Center, 538 p.

Dalrymple, R.W., and Choi, K., 2007, Morphologic and facies trends through the fluvial-marine transition in tide-dominated depositional systems: A schematic framework for environmental and sequence-stratigraphic interpretation: Earth-Science Reviews, v. 81, p. 135–174, https://doi.org/10.1016/j.earscirev.2006.10.002.

Dalrymple, R.W., Baker, E.K., Harris, P.T., and Hughes, M., 2003, Sedimentology and stratigraphy of a tide-dominated, foreland-basin delta (Fly River, Papua New Guinea), *in* Sidi, F.H., et al., eds., Tropical Deltas of Southeast Asia—Sedimentology, Stratigraphy, and Petroleum Geology: Society of Sedimentary Geology (SEPM) Special Publication 76, p. 147–173, https://doi.org/10.2110/pec.03.76.0147.

Dalrymple, R.W., Kurcinka, C., Jablonski, B., Ichaso, A., and Mackay, D., 2015, Deciphering the relative importance of fluvial and tidal processes in the fluvial-marine transition, *in* Ashworth, P.J., Best, J.L., and Parsons, D.R., eds., Fluvial-Tidal Sedimentology: Developments in Sedimentology 68, p. 3–45, https://doi.org/10.1016/B978-0-444-63529-7.00002-X.

Fox, J.M., Hill, P.S., Milligan, T.G., and Boldrin, A., 2004, Flocculation and sedimentation on the Po River Delta: Marine Geology, v. 203, p. 95–107, https://doi.org/10.1016/S0025-3227(03)00332-3.

Gugliotta, M., and Saito, Y., 2019, Matching trends in channel width, sinuosity, and depth along the fluvial to marine transition zone of tide-dominated river deltas: The need for a revision of depositional and hydraulic models: Earth-Science Reviews, v. 191, p. 93–113, https://doi.org/10.1016/j.earscirev.2019.02.002.

Hanegan, K., and Georgiou, I., 2015, Tidal modulated flow and sediment flux through Wax Lake Delta distributary channels: Implications for delta development: Proceedings of the International Association of Hydrological Sciences, v. 367, p. 367–391, https://doi.org/10.5194/piahs-367-391-2015.

Jaeger, J.M., and Nittrouer, C.A., 1995, Tidal controls on the formation of fine-scale sedimentary strata near the Amazon River mouth: Marine Geology, v. 125, p. 259–281, https://doi.org/10.1016/0025-3227(95)00015-Q.

James, N.P., and Dalrymple, R.W., 2010, Facies Models 4: St. John's, Newfoundland, Canada, Geological Association of Canada, 574 p.

Lamb, M.P., Nittrouer, J.A., Mohrig, D., and Shaw, J., 2012, Backwater and river plume controls on scour upstream of river mouths: Implications for fluvio-deltaic morphodynamics: Journal of Geophysical Research: Earth Surface, v. 117, F01002, https://doi.org/10.1029/2011JF002079 .

Longhitano, S.G., Mellere, D., Steel, R.J., and Ainsworth, R.B., 2012, Tidal depositional systems in the rock record: A review and new insights: Sedimentary Geology, v. 279, p. 2–22, https://doi.org/10.1016/j.sedgeo.2012.03.024.

Macquaker, J.H.S., Bentley, S.J., and Bohacs, K.M., 2010, Wave-enhanced sediment-gravity flows and mud dispersal across continental shelves: Reappraising sediment transport processes operating in ancient mudstone successions: Geology, v. 38, p. 947–950, https://doi.org/10.1130/G31093.1.

Maicu, F., De Pascalis, F., Ferrarin, C., and Umgiesser, G., 2018, Hydrodynamics of the Po River Delta–sea system: Journal of Geophysical Research: Oceans, v. 123, p. 6349–6372, https://doi.org/10.1029/2017JC013601.

Milligan, T.G., Hill, P.S., and Law, B.A., 2007, Flocculation and the loss of sediment from the Po River plume: Continental Shelf Research, v. 27, p. 309–321, https://doi.org/10.1016/j.csr.2006.11.008.

Olariu, C., Steel, R.J., Olariu, M.I., and Choi, K., 2015, Facies and architecture of fluvial-tidal channels (inclined heterolithic strata) of the Campanian Neslen Formation, Utah, USA, *in* Ashworth, P.J., Best, J.L., and Parsons, D.R., eds., Fluvial-Tidal Sedimentology: Developments in Sedimentology 68, p. 353–394, https://doi.org/10.1016/B978-0-444-63529-7.00011-0.

Passey, Q.R., Bohacs, K.M., Esch, W.L., Klimentides, R., and Sinha, S., 2010, From oil-prone source rock to gas-producing shale reservoir—Geological and petrophysical characterization of unconventional shale gas reservoirs: Proceedings of the International Oil and Gas Conference in China, June 2010: Beijing, China, Society of Petroleum Engineers, SPE 131350-MS, p. 29.

Peng, Y., Steel, R.J., and Olariu, C., 2018, Amazon fluid mud impact on tide- and wave-dominated Pliocene lobes of the Orinoco Delta: Marine Geology, v. 406, p. 57–71, https://doi.org/10.1016/j.margeo.2018.08.009.

Rossi, V.M., Kim, W., Leva López, J., Edmonds, D., Geleynse, N., Olariu, C., Steel, R.J., Hiatt, M., and Passalacqua, P., 2016, Impact of tidal currents on delta-channel deepening, stratigraphic architecture, and sediment bypass beyond the shoreline: Geology, v. 44, p. 927–930, https://doi.org/10.1130/G38334.1.

Shaw, J.B., and Mohrig, D., 2014, The importance of erosion in distributary channel network growth, Wax Lake Delta, Louisiana, USA: Geology, v. 42, p. 31–34, https://doi.org/10.1130/G34751.1.

Syvitski, J.P.M., Kettner, A.J., Correggiari, A., and Nelson, B.W., 2005, Distributary channels and their impact on sediment dispersal: Marine Geology, v. 222, p. 75–94, https://doi.org/10.1016/j.margeo.2005.06.030.

Tesi, T., Miserocchi, S., Goñi, M.A., Turchetto, M., Langone, L., De Lazzari, A., Albertazzi, S., and Correggiari, A., 2011, Influence of distributary channels on sediment and organic matter supply in event-dominated coastal margins: The Po prodelta as a study case: Biogeosciences, v. 8, p. 365–385, https://doi.org/10.5194/bg-8-365-2011.

Traykovski, P., Wiberg, P.L., and Geyer, W.R., 2007, Observations and modeling of wave-supported sediment gravity flows on the Po prodelta and comparison to prior observations from the Eel shelf: Continental Shelf Research, v. 27, p. 375–399, https://doi.org/10.1016/j.csr.2005.07.008.

Wheatcroft, R.A., Stevens, A.W., Hunt, L.M., and Milligan, T.G., 2006, The large-scale distribution and internal geometry of the fall 2000 Po River flood deposit: Evidence from digital X-radiography: Continental Shelf Research, v. 26, p. 499–516, https://doi.org/10.1016/j.csr.2006.01.002.

Williams, G.E., 1991, Upper Proterozoic tidal rhythmites, South Australia: Sedimentary features, deposition, and implications for the Earth's paleorotation, *in* Smith, D.G., et al., eds., Clastic Tidal Sedimentology: Canadian Society of Petroleum Geologists Memoir 16, p. 161–178.

Printed in USA